Title

Host and Microbe Blood Metagenomics Reveals Key Pathways Characterizing Critical Illness Phenotypes.

Journal

American Journal of Respiratory and Critical Care Medicine, 209(7)

Authors

Neyton, Lucile
Sinha, Pratik
Sarma, Aartik
et al.

Publication Date

2024-04-01

DOI

10.1164/rccm.202308-1328OC

Peer reviewed

ORIGINAL ARTICLE

Host and Microbe Blood Metagenomics Reveals Key Pathways Characterizing Critical Illness Phenotypes

Lucile P. A. Neyton[1], Pratik Sinha[7], Aartik Sarma[1], Eran Mick[1,2,8], Katrina Kalantar[9], Stephanie Chen[3], Nelson Wu[1], Kevin Delucchi[4], Hanjing Zhuo[5], Lieuwe D. J. Bos[10], Alejandra Jauregui[3], Antonio Gomez[3,11], Carolyn M. Hendrickson[11], Kirsten N. Kangelaris[3], Aleksandra Leligdowicz[12], Kathleen D. Liu[5], Michael A. Matthay[6], Charles R. Langelier[2,8*], and Carolyn S. Calfee[1,5,6*]

[1]Division of Pulmonary, Critical Care, Allergy and Sleep Medicine, [2]Division of Infectious Diseases, [3]Department of Medicine, [4]Department of Psychiatry and Behavioral Sciences, [5]Department of Anesthesiology, and [6]Cardiovascular Research Institute, University of California, San Francisco, San Francisco, California; [7]Department of Anesthesiology, Washington University in St. Louis, St. Louis, Missouri; [8]Chan Zuckerberg Biohub, San Francisco, California; [9]Chan Zuckerberg Initiative, Redwood City, California; [10]Department of Intensive Care and Laboratory of Experimental Intensive Care and Anesthesiology, Academic Medical Center, Amsterdam, the Netherlands; [11]Department of Medicine, Zuckerberg San Francisco General Hospital and Trauma Center, San Francisco, California; and [12]Department of Medicine, University of Toronto, Toronto, Ontario, Canada

ORCID IDs: 0000-0003-1273-2228 (L.P.A.N.); 0000-0002-7299-808X (E.M.); 0000-0001-6055-4644 (A.L.).

Abstract

Rationale: Two molecular phenotypes of sepsis and acute respiratory distress syndrome, termed hyperinflammatory and hypoinflammatory, have been consistently identified by latent class analysis in numerous cohorts, with widely divergent clinical outcomes and differential responses to some treatments; however, the key biological differences between these phenotypes remain poorly understood.

Objectives: We used host and microbe metagenomic sequencing data from blood to deepen our understanding of biological differences between latent class analysis–derived phenotypes and to assess concordance between the latent class analysis–derived phenotypes and phenotypes reported by other investigative groups (e.g., Sepsis Response Signature [SRS1–2], molecular diagnosis and risk stratification of sepsis [MARS1–4], reactive and uninflamed).

Methods: We analyzed data from 113 patients with hypoinflammatory sepsis and 76 patients with hyperinflammatory sepsis enrolled in a two-hospital prospective cohort study. Molecular phenotypes had been previously assigned using latent class analysis.

Measurements and Main Results: The hyperinflammatory and hypoinflammatory phenotypes of sepsis had distinct gene expression signatures, with 5,755 genes (31%) differentially expressed. The hyperinflammatory phenotype was associated with elevated expression of innate immune response genes, whereas the hypoinflammatory phenotype was associated with elevated expression of adaptive immune response genes and, notably, T cell response genes. Plasma metagenomic analysis identified differences in prevalence of bacteremia, bacterial DNA abundance, and composition between the phenotypes, with an increased presence and abundance of *Enterobacteriaceae* in the hyperinflammatory phenotype. Significant overlap was observed between these phenotypes and previously identified transcriptional subtypes of acute respiratory distress syndrome (reactive and uninflamed) and sepsis (SRS1–2). Analysis of data from the VANISH trial indicated that corticosteroids might have a detrimental effect in patients with the hypoinflammatory phenotype.

Conclusions: The hyperinflammatory and hypoinflammatory phenotypes have distinct transcriptional and metagenomic features that could be leveraged for precision treatment strategies.

Keywords: sepsis; transcriptomics; pathogens; phenotypes

(Received in original form August 1, 2023; accepted in final form January 8, 2024)

*Co–senior authors.

Supported by NIH grants 1R35 HL140026 (C.S.C.), K23HL138461-01A1 and 5R01HL155418 (C.R.L.), and R35 GM142992 (P.S.) and by Chan Zuckerberg Biohub.

Author Contributions: Clinical data collection and adjudication: A.J., A.G., C.M.H., K.N.K., A.L., K.D.L., M.A.M., and C.S.C. Analysis plan: L.P.A.N., P.S., E.M., L.D.J.B., C.R.L., and C.S.C. Data processing: L.P.A.N., P.S., E.M., K.K., S.C., N.W., K.D., H.Z., and L.D.J.B. Data analysis: L.P.A.N. and A.S. Interpretation and manuscript drafting: L.P.A.N., S.C., C.R.L., and C.S.C. Manuscript review: All authors.

Data and code availability: The processed gene counts are available from the Gene Expression Omnibus under accession GSE236892. FASTQ sequencing files are protected due to institutional review board protocol restrictions and, therefore, cannot be made publicly available. Scripts used for the analyses are available on GitHub (https://github.com/lucile-n/EARLI_sepsis_LCA/).

Correspondence and requests for reprints should be addressed to Lucile P.A. Neyton, Ph.D., Division of Pulmonary, Critical Care, Allergy and Sleep Medicine, University of California, San Francisco, 505 Parnassus Avenue, #M1083, San Francisco, CA 94143-0111. E-mail: lucile.neyton@ucsf.edu.

Am J Respir Crit Care Med Vol 209, Iss 7, pp 805–815, Apr 1, 2024

Originally Published in Press as DOI: 10.1164/rccm.202308-1328OC on January 8, 2024
Internet address: www.atsjournals.org

To date, despite hundreds of clinical trials in acute respiratory distress syndrome (ARDS) and sepsis, few pharmacologic therapies have demonstrated a consistent or generalizable improvement in disease trajectory or outcome, and treatment remains supportive, with high mortality rates (1). This dismal track record has been attributed in part to the considerable clinical and biological heterogeneity within ARDS and sepsis (2). Two phenotypes of ARDS have been identified using latent class analysis (LCA) applied to clinical and plasma protein biomarker data in six randomized controlled trials (3–7) (RCTs) and, more recently, in two observational cohorts (8). These phenotypes, termed hyperinflammatory and hypoinflammatory, have distinct biological features and outcomes. The hyperinflammatory phenotype is characterized by higher levels of circulating proinflammatory biomarkers and higher mortality, relative to the hypoinflammatory phenotype. Additionally, when stratifying by phenotype, differential treatment responses were observed in three secondary analyses of RCT data (3–5), suggesting that these LCA-derived phenotypes may represent treatable traits. Our group recently reported that these phenotypes are also identifiable in sepsis and appear to respond differently to activated protein C (9). These findings, along with those of a previous study (10), suggest that the hyperinflammatory and hypoinflammatory phenotypes are shared between sepsis and ARDS.

Although the consistency of these phenotypes across critical illness syndromes suggests new potential therapeutic directions in the field, the key biological pathways distinguishing them remain incompletely understood, representing a major barrier to identifying and testing novel phenotype-specific therapies. Higher levels of plasma proteins related to systemic inflammation, dysregulated endothelial responses, and coagulopathy in the hyperinflammatory phenotype suggest that pathogen burden may also differ markedly. This idea is supported by our observation of a higher prevalence of bacteremia in the hyperinflammatory phenotype (9). Despite this, our understanding of whether sepsis phenotypes are driven by specific underlying pathogens has remained limited.

Several groups have identified sepsis and ARDS phenotypes using either only transcriptional profiling (Sepsis Response Signature [SRS1–2], molecular diagnosis and risk stratification of sepsis [MARS1–4]) or only protein biomarkers (reactive and uninflamed) (11–13). The extent to which these phenotypes overlap with the hyperinflammatory and hypoinflammatory phenotypes in sepsis has been unknown and could provide insight into the generalizability of phenotypes across critical illness syndromes. Previous studies, including analyses of sepsis (14) and LCA-derived coronavirus disease (COVID-19) ARDS (15) phenotypes, highlighted differential treatment responses to corticosteroids. Determining whether differential response to corticosteroids is also a feature of the hyperinflammatory and hypoinflammatory sepsis phenotypes could shed light on phenotype generalizability and inform therapeutic strategies with the potential to benefit certain patient subgroups.

The primary objective of this study was to compare the biological profiles of the two LCA-derived hyperinflammatory and hypoinflammatory sepsis phenotypes using whole blood transcriptional profiling and plasma metagenomic sequencing of circulating microbial DNA. We also sought to compare these sepsis phenotypes to other previously identified phenotypes of ARDS and sepsis to assess the concordance of different phenotyping approaches across syndromic definitions of disease. Last, we evaluated phenotype-specific treatment response to corticosteroids.

Some of the data in this article have been previously included in a published study (16).

Methods

Clinical Cohort and Data

For this analysis, we selected patients who developed sepsis, defined as suspected or confirmed infection with at least two systemic inflammatory response syndrome criteria (e.g., sepsis-2 criteria), from the Early Assessment of Renal and Lung Injury (EARLI) observational cohort (*see* Supplementary Methods in the online supplement). For practical reasons, subjects who were intubated and/or hypotensive in the emergency department (ED) were preferentially selected for PAXgene tube collection and, therefore, for sequencing (*see* Table E1 in the online supplement). Sepsis phenotypes were assigned using LCA as previously reported (9).

Whole blood samples were collected in PAXgene tubes and utilized for sequencing. We used kallisto (17) to generate gene counts (Supplementary Methods).

Gene Expression Differences

We studied differences in gene expression between LCA-derived hyperinflammatory and hypoinflammatory sepsis phenotypes by performing a differential expression analysis using DESeq2 (18) in R (Supplementary Methods). The analysis was reproduced using the fraction of absolute neutrophil count per white blood cell count as an additional covariate to assess if the differences in gene expression profiles between the phenotypes were driven by differences in neutrophil proportions. Gene ranks were compared using Spearman's correlation coefficient and individual gene statistics.

To identify biological terms of interest, we performed a pathway analysis using Ingenuity Pathway Analysis (QIAGEN; https://digitalinsights.qiagen.com/products-overview/discovery-insights-portfolio/analysis-and-visualization/qiagen-ipa/). To assess the results' consistency, we additionally performed a gene set enrichment analysis (19) using the list of genes ranked based on fold-change values and the Reactome database of gene sets (20) (Supplementary Methods).

To infer cell-type fractions from bulk gene expression data, we used CIBERSORTx and the LM22 reference matrix (21), listing 22 types of human cell phenotypes (Supplementary Methods).

Microbial Differences

DNA sequencing was performed on plasma samples stored in ethylenediaminetetraacetic acid tubes. Sequencing data were processed using the IDseq pipeline (22). A rules-based model, identifying overrepresented pathogens in metagenomic data, was used to flag pathogens (16). The abundance of bacterial species was estimated using the normalized number of reads mapping to a given species. Data were aggregated at the species level using phyloseq in R and

This article has a related editorial.

This article has an online supplement, which is accessible from this issue's table of contents at www.atsjournals.org.

At a Glance Commentary

Scientific Knowledge of the Subject: Despite numerous clinical trials in acute respiratory distress syndrome (ARDS) and sepsis, few pharmacologic therapies have consistently improved outcomes, attributing the challenges to the clinical and biological heterogeneity within these conditions. Latent class analysis (LCA) identified two ARDS and sepsis phenotypes, hyperinflammatory and hypoinflammatory, marked by distinct features and outcomes. These phenotypes exhibit differential treatment responses, suggesting treatable traits. As potential therapeutic directions emerge, the underlying biological pathways and pathogen contributions remain unclear, hindering the development of phenotype-specific therapies.

What This Study Adds to the Field: This study delves into the biological foundations of two sepsis phenotypes, revealing distinct host and microbial characteristics. The hyperinflammatory phenotype exhibits heightened innate immunity and metabolic gene expression, paralleled by an increased abundance of bacterial DNA in the blood. Conversely, the hypoinflammatory phenotype is marked by T-cell signaling, suggesting a link between immunosuppression, metabolic dysfunction, and poor outcomes. Notably, the study exposes a breach in the traditional concept of a sterile bloodstream in sepsis, with patients with the hyperinflammatory phenotype showing greater bacteremia and compositional differences. The partial overlap with established phenotypes emphasizes the complexity of critical illness, urging further efforts to consolidate and understand diverse phenotyping schemas. These findings contribute to refining biomarkers for therapeutic targeting and hold implications for predictive enrichment in clinical trials for critical conditions.

taxonomic information from the National Center for Biotechnology Information database (23). The Bray-Curtis dissimilarity measure was used to assess differences in β diversity between samples and the adonis2 function from the vegan package to compute the associated *P* value using PERMANOVA. Differential abundance analysis was performed using Wilcoxon tests.

Comparison with Previously Described Phenotypes

To study the similarities between the hyperinflammatory and hypoinflammatory phenotypes and previously described subtypes of sepsis—SRS1 and SRS2 from the GAinS study (13), sepsis MARS1–4 from the MARS cohort (11), and ARDS and sepsis reactive and uninflamed from the MARS study (12)—we compared the hyperinflammatory and hypoinflammatory fold changes in EARLI to the fold changes for the SRS, MARS, and reactive and uninflamed subtypes in the external cohorts. More specifically, we matched each of the two phenotypes of interest to one of the external phenotypes, on the basis of clinical similarities, and compared gene expression fold changes. For the MARS1–4 comparison, we considered all possible phenotype pairs to identify the groups being the most similar to the hyperinflammatory and hypoinflammatory phenotypes. Normalized gene expression values were collected, respectively, from the ArrayExpress database (E-MTAB-4421 and E-MTAB-4451) and the Gene Expression Omnibus website (GSE65682; Supplementary Methods). Spearman's correlation coefficient was chosen to perform the comparison. Ninety-five percent Wilson confidence intervals (24) were generated (Supplementary Methods).

Differential Therapeutic Responses

Array-based gene expression data from the VANISH trial of septic shock (25) were collected from ArrayExpress (E-MTAB-7581). Support vector machine–based classifiers (26) were built with the Python scikit-learn (27) library. This model was then applied to patients with transcriptomic data ($N = 117$) from the VANISH trial to allocate patients to the hyperinflammatory or hypoinflammatory phenotype. A logistic regression model was used to test for phenotype-specific treatment effect (Supplementary Methods).

Results

Clinical Cohort and Data

We studied a subset of 189 intubated and/or hypotensive patients with sepsis (*see* Figure E1 in the online supplement) who were enrolled in the EARLI prospective cohort study at two hospitals affiliated with the University of California, San Francisco (Table E1). Samples were collected at a median time of 15 hours after ED admission (Table E1) (28). Demographics, clinical features, plasma protein biomarker measurements, and outcomes are presented in Table 1. Differences between phenotypes were consistent with previous analyses of LCA-derived phenotypes in ARDS and sepsis (9). (For additional characteristics, *see* Table E2 in the online supplement; for a summary of the missing data, *see* Table E3 in the online supplement.)

Gene Expression Differences

We first assessed biological differences between the two sepsis phenotypes on the basis of differential gene expression analysis using DESeq2 (18). Of the 18,354 genes compared, 5,755 (31%) were found to be differentially expressed at a false discovery rate threshold of 0.05 (Figure 1A). These findings were consistent after adjusting for the fraction of absolute neutrophil count per white blood cell count (Spearman's $R = 0.92$), which was significantly higher in the hyperinflammatory phenotype (Table 1).

On the basis of these differentially expressed genes, we sought to identify associated pathways enriched in each phenotype using Ingenuity Pathway Analysis. Thirty-one pathways were found to be significantly enriched (absolute Z score > 2; Figure 1B). Gene set enrichment analysis using the Reactome database produced similar results (File E1).

Overall, the hyperinflammatory phenotype was characterized by the activation of pathways related to the innate immune response and energy metabolism, including oxidative phosphorylation, glycolysis, and cholesterol biosynthesis pathways. Immune response pathways also showed elevated expression in patients with the hyperinflammatory phenotype, including the PD-1, PD-L1 cancer immunotherapy, MSP-RON, and IL-8 signaling pathways. Additionally, several cell motility pathways known to be essential for innate immune responses (29), such as

Table 1. Cohort Characteristics

Characteristic	All Included (*N* = 189)	Hypo (*n* = 113)	Hyper (*n* = 76)	*P* for Hyper vs. Hypo
Age, yr, mean (SD)	65 (15)	65 (15)	66 (15)	0.73*
Gender, *n* (%)				0.70†
Male	112 (59)	66 (58)	46 (61)	—
Female	76 (40)	46 (41)	30 (39)	—
Transgender	1 (1)	1 (1)	0 (0)	—
Race, *n* (%)				0.82†
White	71 (38)	42 (37)	29 (38)	—
Asian	58 (31)	35 (31)	23 (30)	—
Black	34 (18)	22 (19)	12 (16)	—
Other	23 (12)	12 (11)	11 (14)	—
NA	3 (2)	2 (2)	1 (1)	—
BMI, mean (SD)	26.3 (8.8)	26.8 (9.4)	25.4 (7.8)	0.30*
Temperature, °C, mean (SD)	37.9 (1.4)	37.9 (1.2)	37.8 (1.6)	0.80*
Heart rate, beats/min, mean (SD)	128 (27)	124 (25)	134 (30)	0.01*
SBP, mm Hg, mean (SD)	82 (20)	87 (21)	75 (15)	<0.001*
Pa_{CO_2}, mm Hg, mean (SD)	43 (19)	47 (21)	38 (14)	<0.001*
Pa_{O_2}/Fi_{O_2}, mm Hg, median (Q1–Q3)	168 (101–279)	175 (114–304)	151 (78–261)	0.09‡
Respiratory rate, breaths/min, mean (SD)	35 (8)	34 (8)	36 (8)	0.12*
Hematocrit, %, mean (SD)	30 (7)	32 (7)	27 (6)	<0.001*
White cell count, 10^3/μl, median (Q1–Q3)	13 (9–19)	13 (10–17)	14 (8–22)	0.44‡
ANC/WBCs, %, median (Q1–Q3)	86 (76–92)	83 (73–90)	90 (83–94)	<0.001‡
Platelets, 10^3/μl, median (Q1–Q3)	151 (85–229)	193 (137–251)	84 (40–141)	<0.001‡
Sodium, mmol/L, mean (SD)	135 (6)	137 (6)	133 (6)	<0.001*
Creatinine, mg/dl, median (Q1–Q3)	1.4 (1–2.4)	1.1 (0.7–1.8)	2 (1.3–3.1)	<0.001‡
Bicarbonate, mmol/L, mean (SD)	20 (7)	23 (6)	16 (5)	<0.001*
Albumin, g/dl, mean (SD)	2.4 (0.7)	2.7 (0.6)	2.1 (0.6)	<0.001*
Bilirubin, (mg/dl, median (Q1–Q3)	1 (0.6–1.5)	0.7 (0.4–1.2)	1.3 (0.9–2.4)	<0.001‡
Vasopressor use at enrollment, *n* (%)				
Yes	152 (80)	79 (70)	73 (96)	<0.001†
Mechanical ventilation at enrollment, *n* (%)				
Yes	162 (86)	101 (89)	61 (80)	0.12†
Primary source of sepsis, *n* (%)				<0.001‡
Pulmonary	104 (55)	76 (67)	28 (37)	—
Nonpulmonary	68 (36)	29 (26)	39 (51)	—
Unclear	17 (9)	8 (7)	9 (12)	—
Bacteremia, *n* (%)				<0.001†
Yes	46 (24)	9 (8)	37 (49)	—
Berlin ARDS, *n* (%)				<0.01†
Yes	88 (47)	43 (38)	45 (59)	—
No	64 (34)	47 (42)	17 (22)	—
Other§	37 (20)	23 (20)	14 (18)	—
APACHE III, mean (SD)	115 (37)	101 (30)	135 (39)	<0.001*
In-hospital mortality to Day 60, *n* (%)				
Yes	76 (40)	28 (25)	38 (50)	<0.001†

Definition of abbreviations: ANC = absolute neutrophil count; APACHE III = Acute Physiology and Chronic Health Evaluation III; ARDS = acute respiratory distress syndrome; BMI = body mass index; Hyper = hyperinflammatory phenotype; Hypo = hypoinflammatory phenotype; NA = not applicable; Q1 = first quartile; Q3 = third quartile; SBP = systolic blood pressure; WBCs = white blood cells.
Demographics and clinical outcomes are presented for the 189 selected samples. Values by phenotype label are presented, and differences between the two phenotypes are tested for. For continuous variables, the mean or median and (SD or Q1–Q3) are reported. For categorical variables, the numbers of patients falling into the different categories are reported. Corresponding (percentages) are reported as well.
**t* test.
†Chi-square test.
‡Mann-Whitney test.
§Other indicates patients for which ARDS status could not be determined because of an underlying condition, a cardiac arrest, or an equivocal chest X-ray that prevented the establishment of status.

RHOA and Rho signaling, were enriched in patients with the hyperinflammatory phenotype.

In contrast, patients with the hypoinflammatory phenotype exhibited increased expression of genes related to T cell responses, including CD28; Th1 and Th2; nuclear factor of activated T cells, or NFAT; protein kinase C; ICOS-ICOSL; and T cell receptor signaling.

In silico analysis of cell type proportions using CIBERSORTx (21) (Figure 1C) predicted increased proportions of innate immune cells, including macrophages, mast cells, dendritic cells, and natural killer cells, in patients with the hyperinflammatory phenotype. Adaptive immune cells, including T cells and plasma cells, were found in greater proportions in patients with the hypoinflammatory phenotype.

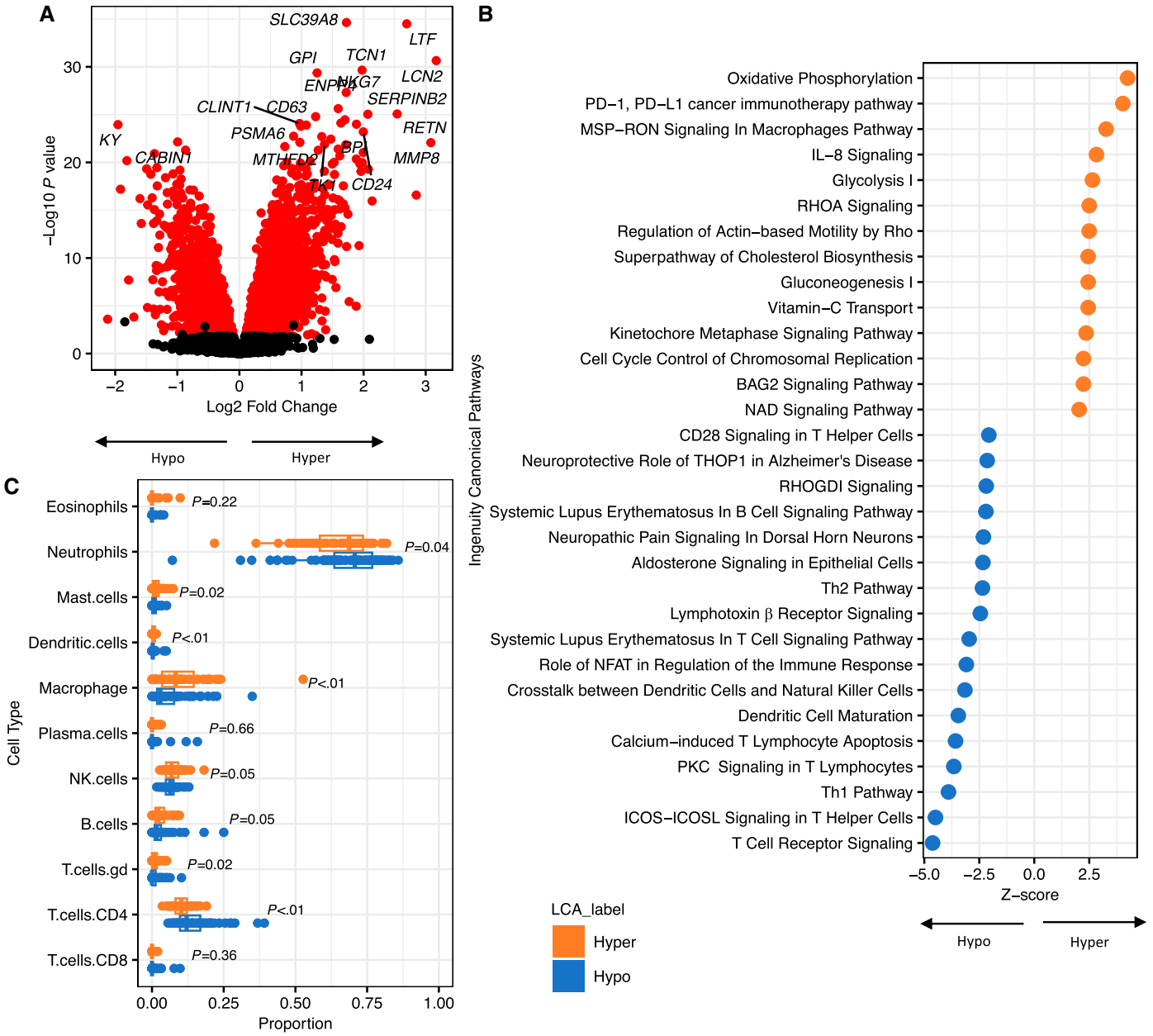

Figure 1. Gene expression differences between phenotypes identified by transcriptional profiling. (*A*) Volcano plot highlighting differentially expressed genes between hyperinflammatory and hypoinflammatory phenotypes. Log_2 fold change values are reported on the *x*-axis. $-Log_{10}$ *P* values are represented on the *y*-axis. Each circle marker corresponds to a gene. Red dots indicate genes significantly differentially expressed. The top 25 (ordered by adjusted *P* value) differentially expressed genes are highlighted. (*B*) Enriched pathways based on differentially expressed genes between hyperinflammatory and hypoinflammatory phenotypes. Pathways were selected on the basis of *Z* score and *P* value and ordered given their *Z* score, which is represented on the *x*-axis. All significant pathways are represented. *Z*-score values quantify the overlap between differentially expressed genes and a given gene set. *Z*-score values also incorporate the direction of expression. Pathway terms are listed on the *y*-axis. The color of each dot represents the direction of the enrichment; a positive value represents a term enriched in the hyperinflammatory phenotype, and a negative value represents a term enriched in the hypoinflammatory phenotype. All reported terms were significantly enriched (absolute *Z* score > 2). (*C*) *In silico* deconvolution on the basis of the LM22 signature. Cell type proportions between the phenotypes for 11 types of cells are represented (*x*-axis). The different types of cells are listed on the *y*-axis. Adjusted *P* values are reported. Differences were tested for using Wilcoxon tests and Benjamini-Hochberg adjustments for multiple comparisons. gd = gamma delta; Hyper = hyperinflammatory phenotype; Hypo = hypoinflammatory phenotype; LCA = latent class analysis; NFAT = nuclear factor of activated T cells; NK = natural killer; PKC = protein kinase C.

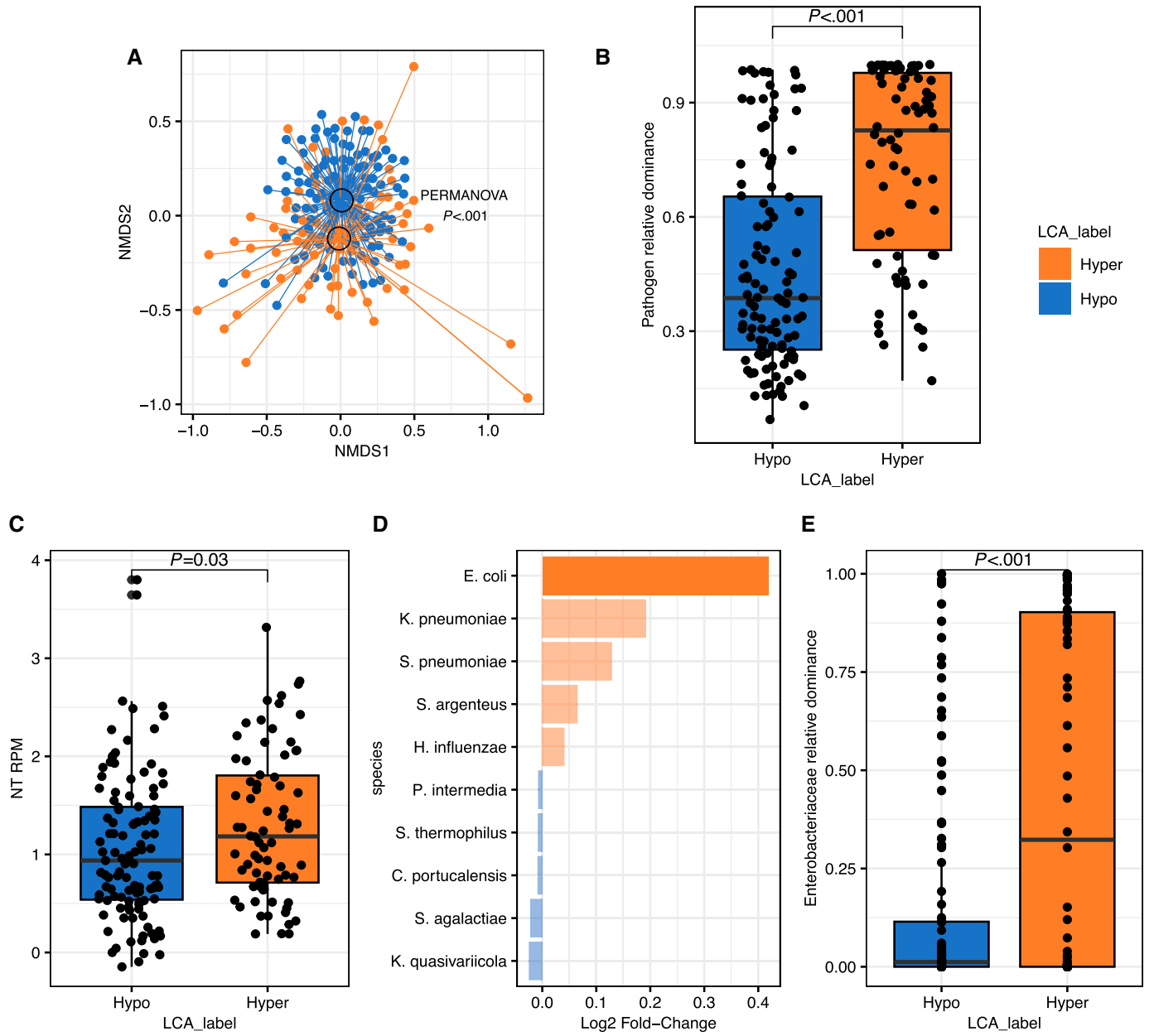

Figure 2. Microbial differences between sepsis phenotypes identified by plasma metagenomics. (*A*) Nonmetric multidimensional scaling-reduced representation of Bray-Curtis distances demonstrating potential plasma bacterial compositional differences between the hyperinflammatory (Hyper; orange; $n = 74$) and hypoinflammatory (Hypo; blue; $n = 111$) phenotypes. (*B*) The relative dominance of the most abundant pathogen detected by plasma metagenomics in hyperinflammatory versus hypoinflammatory phenotypes. Relative dominance represents the proportion of sequencing reads mapping to the most abundant pathogen in each sample relative to all other bacterial genera. The Wilcoxon-derived *P* value is reported. (*C*) Differences in the relative abundance of bacterial pathogens (30, 31) between the hyperinflammatory and hypoinflammatory phenotypes measured in sequencing RPM. The Wilcoxon-derived *P* value is reported. (*D*) Differential abundance analysis of sepsis-associated bacterial pathogens (genus level) detected in plasma from patients with hyperinflammatory versus hypoinflammatory sepsis phenotypes. Log_2 fold-change values for hyperinflammatory vs. hypoinflammatory phenotypes are reported on the *x*-axis. Each one of the top five genera per fold-change direction is a bar on the *y*-axis. Lighter colored bars indicate genera that did not meet the significance threshold of adjusted $P < 0.05$. (*E*) Proportion of total bacterial reads matching to the Enterobacteriaceae family per phenotype. For each patient, represented by a dot, the proportion of total bacterial reads mapping to the Enterobacteriaceae family is reported on the *y*-axis. The Wilcoxon *P* value for the comparison of Hypo to Hyper is reported. LCA = latent class analysis. RPM = reads per million.

A

Cohort name	Condition	Phenotypes of interest	Number of subjects
GAinS	Sepsis	SRS1-2	371
MARS	Sepsis	MARS1-4	479
MARS	Sepsis+ARDS	reactive/uninflamed	364

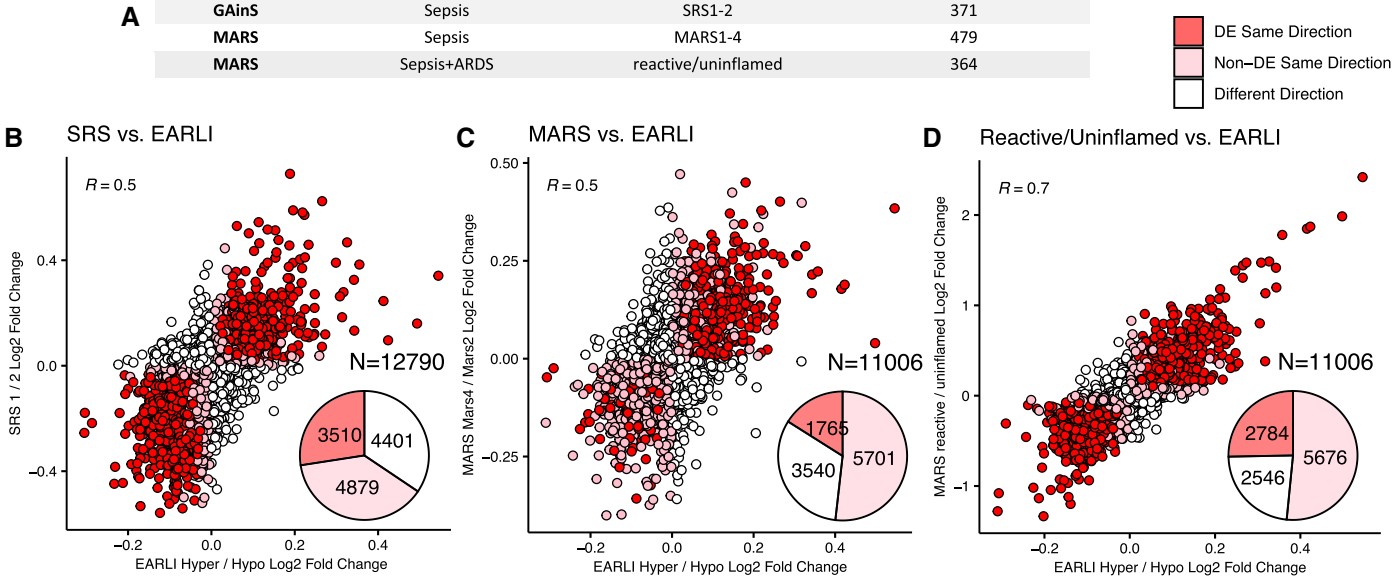

Figure 3. Transcriptional comparison of the Early Assessment of Renal and Lung Injury (EARLI) sepsis phenotypes and other sepsis and/or acute respiratory distress syndrome (ARDS) phenotypes. (*A*) Summary of datasets comparatively evaluated. Each row corresponds to a dataset with described phenotypes of sepsis and/or ARDS. The names of the cohorts, corresponding condition, external phenotype names, and number of subjects with available gene expression data are listed. (*B*) Comparison between EARLI hyperinflammatory and hypoinflammatory phenotypes and the SRS1 and SRS2 phenotypes. Each dot represents a gene measured in GAinS and EARLI cohorts. The *x*-axis coordinates represent the $\log_2$ fold-change values for the comparison of hyperinflammatory with hypoinflammatory phenotypes in EARLI. The *y*-axis coordinates represent the $\log_2$ fold-change values for SRS1 versus SRS2. On the *y*-axis, positive values represent genes that are overexpressed in SRS1 when compared with SRS2. Spearman's correlation coefficients (R) are reported. Pie charts represent a comparison of DE genes. (*C*) Comparison of EARLI hyperinflammatory and hypoinflammatory phenotypes with the MARS4 and MARS2 phenotypes. (*D*) Comparison between EARLI hyperinflammatory and hypoinflammatory phenotypes and the reactive and uninflamed phenotypes. DE = differentially expressed.

Microbial Differences

Next, we used plasma metagenomic DNA sequencing ($n = 185$) to compare microbial composition between the hyperinflammatory and hypoinflammatory phenotypes. Bray-Curtis dissimilarity suggested significant differences in β diversity between phenotypes (PERMANOVA, <0.001) (Figure 2A). Microbial alignments from the hyperinflammatory phenotype were more often characterized by dominance of a single bacterial species (median read proportion of highest represented species, 0.83 vs. 0.39; Wilcoxon $P < 0.001$) (Figure 2B).

We next used a previously established metagenomic rules-based model (16) to identify probable sepsis pathogens (30, 31) in the plasma metagenomics data. The performance characteristics of this model with respect to a gold standard of bacterial culture in this population were recently described (16). As previously reported, we found that agreement with culture-based microbiologic testing varied by species and sampling site (*see* Table E4 in the online supplement).

We found a higher abundance of bacteria, measured in bacterial reads per million, in plasma from patients with the hyperinflammatory phenotype (Wilcoxon $P = 0.03$; Figure 2C), compared with patients with the hypoinflammatory phenotype. Plasma microbial DNA mass was also significantly higher in patients with the hyperinflammatory phenotype versus those with the hypoinflammatory phenotype (*see* Figure E2 in the online supplement). Differential abundance analysis revealed that *Escherichia coli*, ubiquitous enteric commensals that can act as sepsis pathogens in the bloodstream, were more abundant in patients with the hyperinflammatory phenotype (Figure 2D). To assess whether translocation of enteric organisms might contribute to the immunologic features of the hyperinflammatory phenotype, we calculated the proportion of bacterial reads mapping to *Enterobacteriaceae*. We found that Enterobacteriaceae species were much more abundant in patients with the hyperinflammatory phenotype, supporting the hypothetical role of gut translocation in this phenotype (Figure 2E). The relative paucity of culture-confirmed Enterobacteriaceae in the respiratory tract ($n = 3$) or urinary tract ($n = 3$) further substantiates the hypothesis that the source in blood may be originating from the gut (Table E4).

Comparison with Previously Described Phenotypes

Next, to assess overlap across different phenotype schemas, we sought to compare transcriptional differences between the hyperinflammatory and hypoinflammatory sepsis phenotypes in our cohort to the differences between previously described transcriptomic phenotypes of sepsis, namely MARS1–4 and SRS1–2 (11, 13), as well as to the reactive and uninflamed phenotypes of ARDS and sepsis (12) (Figure 3A).

First, using publicly available data, we compared the LCA-derived hyperinflammatory and hypoinflammatory phenotypes with the SRS1 and SRS2 sepsis phenotypes derived from blood transcriptional profiling in the GAinS

cohort (13). We compared gene expression fold changes among patients in the GAinS cohort (SRS1 vs. SRS2 phenotypes) with gene expression fold changes among patients in the EARLI cohort (hyperinflammatory vs. hypoinflammatory phenotypes; Figure 3B). The correlation between gene expression fold changes in the hyperinflammatory versus hypoinflammatory phenotypes and SRS1 versus SRS2 phenotypes was moderate, with a Spearman's R = 0.5, and a statistically significant Wilson score interval (<0.001, <0.01).

Next, we compared differences in gene expression between the MARS phenotypes (10, 11) and the hyperinflammatory and hypoinflammatory phenotypes. As more than two MARS phenotypes are described, we identified the two phenotypes most closely matching the hyperinflammatory and hypoinflammatory phenotypes on the basis of Spearman's correlation. We determined that the MARS2 and MARS4 phenotypes most closely corresponded with hyperinflammatory and hypoinflammatory phenotypes, respectively, on the basis of the highest correlation value. Comparative evaluation of gene expression between phenotypes (Figure 3C) demonstrated a nonsignificant Spearman's R = 0.5 (Wilson score interval: 0.08, 0.11). Despite this correlation value being identical to the GAinS-derived value, the range of fold changes was narrower and, thus, more likely to occur by chance.

Last, we compared our phenotypes with the reactive and uninflamed sepsis-associated ARDS phenotypes (12). We compared the differences in gene expression between the reactive and uninflamed phenotypes in the MARS cohort with the differences in gene expression between the hyperinflammatory and hypoinflammatory phenotypes, respectively. Correlation between gene expression in the phenotypes was high (Spearman's R = 0.7; Wilson score interval: <0.001, <0.01; Figure 3D), indicating a strong overlap between these independently identified phenotypes. As a sensitivity analysis, we reproduced the aforementioned analyses; that is, comparing gene expression fold-change values between each external phenotyping approach and hyperinflammatory phenotype versus hypoinflammatory phenotype in EARLI, including only genes identified as differentially expressed in EARLI. The conclusions reached were the same (*see* Figure E3 in the online supplement).

For each external phenotyping approach, we independently quantified the enrichment of pathways identified as differentially enriched in the hyperinflammatory phenotype versus the hypoinflammatory phenotype to assess overlap. Comparison of activated and inhibited pathways with the results of our main analysis confirmed the overlap, with 11 out of 31 pathways in common for SRS1 versus SRS2, 6 out of 31 for MARS2 versus MARS4, and 19 out of 31 for reactive versus uninflamed (*see* Figure E4 in the online supplement). Notably, the pathways previously identified as the most activated when comparing the hyperinflammatory phenotype with the hypoinflammatory phenotype (oxidative phosphorylation and PD-1, PD-L1 cancer immunotherapy) were also identified as activated when comparing the reactive phenotype with the uninflamed phenotype.

Differential Therapeutic Responses

Previous studies of LCA-derived ARDS phenotypes have suggested that they may represent treatable traits with phenotype-specific treatment responses (3–5). Likewise, we recently reported that the hyperinflammatory and hypoinflammatory sepsis phenotypes exhibited differential responses to activated protein C in a secondary analysis of the PROWESS-SHOCK dataset (9). We sought to further test the hypothesis that these phenotypes would respond differently to treatment in a secondary analysis of the VANISH trial (25), which tested the effect of randomly assigned vasopressin versus norepinephrine and hydrocortisone versus placebo in patients with septic shock. We used gene expression data from EARLI to create a bagged support vector machine classifier, which was trained and tested using cross-validation in the EARLI dataset to allocate patients in the VANISH trial to the hyperinflammatory or hypoinflammatory phenotype. The resulting area under the receiver operating curve was 0.89 (SD = 0.07). A logistic regression model was then fitted to test for the interaction between phenotype and treatment, and for its effect on 28-day mortality. We found that treatment responses in VANISH significantly differed on the basis of phenotype (interaction $P < 0.01$; Figure E5; *see* Table E5 in the online supplement). The mortality rate was similar for patients with the hyperinflammatory phenotype who were treated with hydrocortisone or placebo (both 41%), but it was higher for patients with the hypoinflammatory phenotype receiving hydrocortisone than for those receiving placebo (44% vs. 10%). This observed interaction was similar to a previously published analysis of the SRS1 and SRS2 phenotypes, which is consistent with a significant overlap between the SRS1 and SRS2 phenotypes and the LCA-derived hyper- and hypoinflammatory phenotypes (14). Additionally, we compared predicted labels to SRS labels and observed a significant overlap between the two phenotyping schemas ($P < 0.001$; *see* Table E6 in the online supplement). We found no evidence of differential treatment effect for vasopressors (vasopressin versus norepinephrine, $P = 0.52$).

Discussion

Our results provide new insights into the biological underpinnings of two established sepsis phenotypes from both host and microbial perspectives. We found that the hyperinflammatory phenotype is characterized by increased expression of innate immunity and metabolism-related genes in the blood, whereas the hypoinflammatory phenotype is enriched in T cell and adaptive immunity signaling pathways. Using plasma metagenomics, we discovered that circulating microbial composition differs between phenotypes, with patients with the hyperinflammatory phenotype characterized by an increased abundance of DNA from bacterial sepsis pathogens. Comparison against external transcriptomic datasets demonstrates conservation of critical illness inflammatory phenotypes across studies, with the hyperinflammatory and hypoinflammatory phenotypes exhibiting significant similarities with the reactive and uninflamed phenotypes of ARDS and sepsis and moderate similarities with the SRS1 and SRS2 sepsis phenotypes, respectively.

We found that increased expression of innate immune genes characterized the hyperinflammatory phenotype; in particular, genes involved in MSP-RON (32) and IL-8 signaling, which is consistent with the increased abundance of plasma IL-8 that is an intrinsic feature of this phenotype (Table E2). Conversely, in patients with the hypoinflammatory phenotype, a strong signal associated with T cell response was identified. This finding supports the

hypothesis that patients with the hyperinflammatory phenotype are characterized by T cell exhaustion and an immunosuppressed phenotype (33). This was also reflected by our *in silico* cell proportion analysis, which demonstrated increased proportions of several T cell populations—in particular, CD4 T cells—in patients with the hypoinflammatory phenotype. The PD-1, PD-L1 cancer immunotherapy pathway, describing inhibition of PD-1 signaling, was the second most enriched pathway in patients with the hyperinflammatory phenotype. PD-1 downregulates T cell activity during immune response, suggesting that patients with the hyperinflammatory phenotype may have attenuated T cell signaling. It is interesting that the inhibition of the PD-1, PD-L1 axis has been proposed as a therapeutic strategy in the treatment of sepsis (34). Indeed, immunosuppression caused by T cell exhaustion has been observed in patients with sepsis, and inhibiting PD-1 signaling might have the potential to partially restore T cell activity. These findings suggest that such a therapeutic strategy might have differential effects in the two LCA-derived phenotypes, pending the results of additional studies examining cell type–specific activity related to PD-1 signaling.

We also found that the hyperinflammatory phenotype was characterized by increased expression of genes associated with energy metabolic pathways. This may reflect increased energy demand of rapidly proliferating immune cell populations—in particular, macrophages—which were predicted to be enriched in the hyperinflammatory phenotype. Given the worse outcomes, metabolic acidosis, and organ dysfunction characteristic of patients with the hyperinflammatory phenotype, these gene expression patterns suggest that metabolic dysfunction may contribute to the pathophysiology inherent to this phenotype. The elevation of lactate levels could be a consequence of an imbalance in energy metabolism. Additionally, in a recent metabolomics study comparing the hyperinflammatory and hypoinflammatory phenotypes, higher lactate levels were observed in patients with the hyperinflammatory phenotype (35). Vitamin C transport was found to be dysregulated as well in the hyperinflammatory phenotype. Conceptually, vitamin C has the potential to reduce mitochondrial dysfunction and inflammation; however, several studies in which it has been trialed as a treatment for sepsis have had mostly disappointing results (36).

Our findings suggest that corticosteroids, through their immunosuppressive effects, might have differential benefits on the basis of the sepsis phenotype. This hypothesis is supported by our observation that patients with the hypoinflammatory phenotype in the VANISH cohort had higher mortality with hydrocortisone treatment, and it is also in line with findings from a previously published analysis of the SRS1 and SRS2 phenotypes (14). A recent study of patients with COVID-19 found that corticosteroids were associated with poor outcomes in those with a previously described hypoinflammatory COVID-19 ARDS phenotype (15), further supporting the idea that steroids may be detrimental in patients with the hypoinflammatory phenotype.

Although the bloodstream has been traditionally considered a sterile environment, this concept is breached in sepsis, where microbial invasion and gut translocation play a direct role in pathogenesis (16, 37, 38). Using metagenomics, we found that bacteremia was more prevalent in patients with the hyperinflammatory phenotype when compared with those with the hypoinflammatory phenotype, supporting our previous culture-based findings (9). Through the novel use of plasma metagenomic sequencing to probe microbial differences between sepsis phenotypes, we found that patients with the hyperinflammatory phenotype had a greater abundance of circulating DNA from bacterial pathogens, as well as differences in the composition of detected bacterial taxa, including a greater proportion of *Enterobacteriaceae* species and, in particular, *Escherichia coli* (which were often also identified in culture-based blood samples). Given that *Enterobacteriaceae* species are classically enteric microbes, these observations suggest that translocation from the gut into the bloodstream might be disproportionately occurring in patients with the hyperinflammatory phenotype (39).

We identified a strong, although incomplete, overlap between the hyperinflammatory and hypoinflammatory sepsis phenotypes and the previously described reactive and uninflamed phenotypes, as well as the SRS1 and SRS2 phenotypes of sepsis and/or ARDS. This finding supports the idea that conserved phenotypes exist across critical illness syndromes. For instance, oxidative phosphorylation and cholesterol biosynthesis were enriched in the same direction in both the hyperinflammatory and reactive phenotypes. Likewise, the hypoinflammatory and uninflamed phenotypes had similar overexpressed pathways, such as T cell signaling, NFAT signaling, and dendritic cell maturation. Overlap in selected biological pathways was also observed between the hyperinflammatory and SRS1 high-risk phenotypes, both of which were marked by transcriptional signatures of adaptive immune suppression. Despite these similarities, it should be noted that the overlap between the transcriptionally derived SRS1 and SRS2 phenotypes and the protein biomarker–derived hypoinflammatory and hyperinflammatory phenotypes was incomplete. This is perhaps, unsurprising, as the reactive and uninflamed phenotypes, like the hyperinflammatory and hypoinflammatory phenotypes, were derived from similar plasma protein biomarkers. These findings suggest that these phenotyping schemas—and, consequently, the data types used to derive them—may offer complementary information to one another, and inclusion of several approaches in future analyses may be of additive value in understanding the heterogeneity of sepsis.

Our study has several strengths. We describe a novel approach to studying sepsis phenotypes by assessing both host and microbial elements using a combination of protein biomarker measurements, transcriptional profiling, and plasma metagenomic sequencing of microbial DNA. All samples were consistently collected early in the hospitalization trajectory, eliminating the risk of bias that would have stemmed from large differences in recruitment times. Additionally, our cohort included patients with diverse demographic characteristics, collected at two different hospitals, each serving unique populations.

This study also has some limitations. The primary analysis was conducted in a single cohort, so findings may not be representative. Similarities in signal observed with several independent cohorts, however, strongly support the hypothesis that our findings are generalizable. It will be crucial to reproduce this analysis in an independent sepsis cohort to refine biomarkers that have the potential to be used as therapeutic targets. In addition, we assessed only the most severely ill patients with sepsis, who were either intubated or on vasopressors in

the ED. The higher severity in our subset of patients might influence gene expression patterns, and future studies reflecting a greater spectrum of sepsis severity will be required. The analysis of differential treatment effect in the VANISH cohort should be interpreted cautiously, as phenotypes were inferred from gene expression data, and there is no validated model or gold standard available at this time. Future studies should seek to prospectively validate these findings.

In conclusion, our analyses have identified biologically plausible and informative differences between LCA-derived hyperinflammatory and hypoinflammatory phenotypes of sepsis at both the gene expression and microbial levels, suggesting that the hyperinflammatory phenotype is characterized by innate immune activation, metabolic dysregulation, and a higher bacterial pathogen burden, compared with the hypoinflammatory phenotype. The partial overlap between these LCA-derived phenotypes and alternative approaches to phenotyping of ARDS and sepsis highlights the ubiquity of informative biological heterogeneity in critical illness and the need for additional efforts to harmonize and synthesize phenotyping schema. Biomarkers associated with genes, pathways, and bacterial profiles highlighted here might be important markers of outcome and treatment response. These findings have implications for the development of therapeutic strategies and, specifically, predictive enrichment in clinical trials of patients with sepsis and other critical illnesses. ■

Author disclosures are available with the text of this article at www.atsjournals.org.

References

1. Boyle AJ, McNamee JJ, McAuley DF. Biological therapies in the acute respiratory distress syndrome. *Expert Opin Biol Ther* 2014;14: 969–981.
2. Laffey JG, Kavanagh BP. Negative trials in critical care: why most research is probably wrong. *Lancet Respir Med* 2018;6:659–660.
3. Calfee CS, Delucchi K, Parsons PE, Thompson BT, Ware LB, Matthay MA; NHLBI ARDS Network. Subphenotypes in acute respiratory distress syndrome: latent class analysis of data from two randomised controlled trials. *Lancet Respir Med* 2014;2:611–620.
4. Famous KR, Delucchi K, Ware LB, Kangelaris KN, Liu KD, Thompson BT, *et al.*; ARDS Network. Acute respiratory distress syndrome subphenotypes respond differently to randomized fluid management strategy. *Am J Respir Crit Care Med* 2017;195:331–338.
5. Calfee CS, Delucchi KL, Sinha P, Matthay MA, Hackett J, Shankar-Hari M, *et al.*; Irish Critical Care Trials Group. Acute respiratory distress syndrome subphenotypes and differential response to simvastatin: secondary analysis of a randomised controlled trial. *Lancet Respir Med* 2018;6:691–698.
6. Sinha P, Delucchi KL, Thompson BT, McAuley DF, Matthay MA, Calfee CS; NHLBI ARDS Network. Latent class analysis of ARDS subphenotypes: a secondary analysis of the statins for acutely injured lungs from sepsis (SAILS) study. *Intensive Care Med* 2018;44:1859–1869.
7. Dahmer MK, Yang G, Zhang M, Quasney MW, Sapru A, Weeks HM, *et al.*; RESTORE and BALI study investigators; Pediatric Acute Lung Injury and Sepsis Investigators (PALISI) Network. Identification of phenotypes in paediatric patients with acute respiratory distress syndrome: a latent class analysis. *Lancet Respir Med* 2022;10:289–297.
8. Sinha P, Delucchi KL, Chen Y, Zhuo H, Abbott J, Wang C, *et al.* Latent class analysis-derived subphenotypes are generalisable to observational cohorts of acute respiratory distress syndrome: a prospective study. *Thorax* 2022;77:13–21.
9. Sinha P, Kerchberger VE, Willmore A, Chambers J, Zhuo H, Abbott J, *et al.* Identifying molecular phenotypes in sepsis: an analysis of two prospective observational cohorts and secondary analysis of two randomised controlled trials. *Lancet Respir Med* 2023;11:965–974.
10. Heijnen NFL, Hagens LA, Smit MR, Cremer OL, Ong DSY, van der Poll T, *et al.* Biological subphenotypes of acute respiratory distress syndrome show prognostic enrichment in mechanically ventilated patients without acute respiratory distress syndrome. *Am J Respir Crit Care Med* 2021; 203:1503–1511.
11. Scicluna BP, van Vught LA, Zwinderman AH, Wiewel MA, Davenport EE, Burnham KL, *et al.*; MARS consortium. Classification of patients with sepsis according to blood genomic endotype: a prospective cohort study. *Lancet Respir Med* 2017;5:816–826.
12. Bos LDJ, Scicluna BP, Ong DSY, Cremer O, van der Poll T, Schultz MJ. Understanding heterogeneity in biologic phenotypes of acute respiratory distress syndrome by leukocyte expression profiles. *Am J Respir Crit Care Med* 2019;200:42–50.
13. Davenport EE, Burnham KL, Radhakrishnan J, Humburg P, Hutton P, Mills TC, *et al.* Genomic landscape of the individual host response and outcomes in sepsis: a prospective cohort study. *Lancet Respir Med* 2016;4:259–271.
14. Antcliffe DB, Burnham KL, Al-Beidh F, Santhakumaran S, Brett SJ, Hinds CJ, *et al.* Transcriptomic signatures in sepsis and a differential response to steroids. From the VANISH randomized trial. *Am J Respir Crit Care Med* 2019;199:980–986.
15. Sinha P, Furfaro D, Cummings MJ, Abrams D, Delucchi K, Maddali MV, *et al.* Latent class analysis reveals COVID-19-related acute respiratory distress syndrome subgroups with differential responses to corticosteroids. *Am J Respir Crit Care Med* 2021;204:1274–1285.
16. Kalantar KL, Neyton L, Abdelghany M, Mick E, Jauregui A, Caldera S, *et al.* Integrated host-microbe plasma metagenomics for sepsis diagnosis in a prospective cohort of critically ill adults. *Nat Microbiol* 2022;7:1805–1816.
17. Bray NL, Pimentel H, Melsted P, Pachter L. Near-optimal probabilistic RNA-seq quantification. *Nat Biotechnol* 2016;34:525–527.
18. Love MI, Huber W, Anders S. Moderated estimation of fold change and dispersion for RNA-seq data with DESeq2. *Genome Biol* 2014;15: 550.
19. Subramanian A, Tamayo P, Mootha VK, Mukherjee S, Ebert BL, Gillette MA, *et al.* Gene set enrichment analysis: a knowledge-based approach for interpreting genome-wide expression profiles. *Proc Natl Acad Sci USA* 2005;102:15545–15550.
20. Fabregat A, Jupe S, Matthews L, Sidiropoulos K, Gillespie M, Garapati P, *et al.* The reactome pathway knowledgebase. *Nucleic Acids Res* 2018; 46:D649–D655.
21. Newman AM, Liu CL, Green MR, Gentles AJ, Feng W, Xu Y, *et al.* Robust enumeration of cell subsets from tissue expression profiles. *Nat Methods* 2015;12:453–457.
22. Kalantar KL, Carvalho T, de Bourcy CFA, Dimitrov B, Dingle G, Egger R, *et al.* IDseq—an open source cloud-based pipeline and analysis service for metagenomic pathogen detection and monitoring. *GigaScience* 2020;9:giaa111.
23. Schoch CL, Ciufo S, Domrachev M, Hotton CL, Kannan S, Khovanskaya R, *et al.* NCBI taxonomy: a comprehensive update on curation, resources and tools. *Database (Oxford)* 2020;2020:baaa062.
24. Wilson EB. Probable inference, the law of succession, and statistical inference. *J Am Stat Assoc* 1927;22:209–212.
25. Gordon AC, Mason AJ, Thirunavukkarasu N, Perkins GD, Cecconi M, Cepkova M, *et al.*; VANISH Investigators. Effect of early vasopressin vs norepinephrine on kidney failure in patients with septic shock: the VANISH randomized clinical trial. *JAMA* 2016;316:509–518.
26. Cortes C, Vapnik V. Support-vector networks. *Mach Learn* 1995;20: 273–297.

27. Pedregosa F, Varoquaux G, Gramfort A, Michel V, Thirion B, Grisel O, *et al.* Scikit-learn: machine learning in Python. *J Mach Learn Res* 2011; 12:2825–2830.
28. Levy MM, Fink MP, Marshall JC, Abraham E, Angus D, Cook D, *et al.*; SCCM/ESICM/ACCP/ATS/SIS. 2001 SCCM/ESICM/ACCP/ATS/SIS International Sepsis Definitions Conference. *Crit Care Med* 2003;31: 1250–1256.
29. Bokoch GM. Regulation of innate immunity by rho GTPases. *Trends Cell Biol* 2005;15:163–171.
30. Weiner-Lastinger LM, Abner S, Edwards JR, Kallen AJ, Karlsson M, Magill SS, *et al.* Antimicrobial-resistant pathogens associated with adult healthcare-associated infections: summary of data reported to the National Healthcare Safety Network, 2015–2017. *Infect Control Hosp Epidemiol* 2020;41:1–18.
31. Magill SS, O'Leary E, Janelle SJ, Thompson DL, Dumyati G, Nadle J, *et al.*; Emerging Infections Program Hospital Prevalence Survey Team. Changes in prevalence of health care-associated infections in U.S. hospitals. *N Engl J Med* 2018;379:1732–1744.
32. Morrison AC, Wilson CB, Ray M, Correll PH. Macrophage-stimulating protein, the ligand for the stem cell-derived tyrosine kinase/RON receptor tyrosine kinase, inhibits IL-12 production by primary peritoneal macrophages stimulated with IFN-γ and lipopolysaccharide. *J Immunol* 2004;172:1825–1832.
33. Fish M, Swanson CM, Shankar-Hari M. Is T cell exhaustion a treatable trait in sepsis? In: Vincent J-L, editor. Annual Update in Intensive Care and Emergency Medicine 2020. Cham, Switzerland: Springer International Publishing; 2020. pp. 271–279.
34. Hotchkiss RS, Monneret G, Payen D. Immunosuppression in sepsis: a novel understanding of the disorder and a new therapeutic approach. *Lancet Infect Dis* 2013;13:260–268.
35. Alipanah-Lechner N, Neyton L, Mick E, Willmore A, Leligdowicz A, Contrepois K, *et al.* Plasma metabolic profiling implicates dysregulated lipid metabolism and glycolytic shift in hyperinflammatory ARDS. *Am J Physiol Lung Cell Mol Physiol* 2023;324:L297–L306.
36. Kashiouris MG, L'Heureux M, Cable CA, Fisher BJ, Leichtle SW, Fowler AA. The emerging role of vitamin C as a treatment for sepsis. *Nutrients* 2020;12:292.
37. Neyton LPA, Langelier CR, Calfee CS. Metagenomic sequencing in the ICU for precision diagnosis of critical infectious illnesses. *Crit Care* 2023; 27:90.
38. Jing Q, Leung CHC, Wu AR. Cell-free DNA as biomarker for sepsis by integration of microbial and host information. *Clin Chem* 2022;68: 1184–1195.
39. Fukuda S, Toh H, Hase K, Oshima K, Nakanishi Y, Yoshimura K, *et al.* Bifidobacteria can protect from enteropathogenic infection through production of acetate. *Nature* 2011;469:543–547.